Icarus 416 (2024) 116100

Contents lists available at ScienceDirect

Icarus

journal homepage: www.elsevier.com/locate/icarus

Subsurface stratigraphy suggested by the layered ejecta craters in the Martian northern planitiae

Sheng Gou [a,b,c], Zongyu Yue [b,c,d], Kaichang Di [b,d,*], Patrick C. Pinet [e], Roberto Bugiolacchi [a,f], Shengli Niu [a,g], Zhanchuan Cai [a], Shuanggen Jin [h,i]

[a] State Key Laboratory of Lunar and Planetary Sciences, Macau University of Science and Technology, Macau 999078, China
[b] State Key Laboratory of Remote Sensing Science, Aerospace Information Research Institute, Chinese Academy of Sciences, Beijing 100101, China
[c] Key Laboratory of Earth and Planetary Physics, Institute of Geology and Geophysics, Chinese Academy of Sciences, Beijing 100029, China
[d] Center for Excellence in Comparative Planetology, Chinese Academy of Sciences, Hefei 230026, China
[e] Institut de Recherche en Astrophysique et Planétologie, Université de Toulouse, CNRS, UPS, CNES, UT3, Toulouse 44346, France
[f] Earth Sciences, University College London, London WC1E 6BT, UK
[g] State Key Laboratory of Space Weather, National Space Science Center, Chinese Academy of Sciences, Beijing 100190, China
[h] Shanghai Astronomical Observatory, Chinese Academy of Sciences, Shanghai 200030, China
[i] School of Surveying and Land Information Engineering, Henan Polytechnic University, Jiaozuo 454003, China

ARTICLE INFO

Keywords:
Layered ejecta craters (LECs)
Martian northern planitiae
Subsurface water-ice
LECs-related strata
High priority regions

ABSTRACT

The formation of layered ejecta craters (LECs) is generally thought to be related to the subsurface water-ice. The distribution of LECs in the northern regions of Mars (0 to 70° N) features both local and latitudinal variations, e.g., there are generally few LECs within volcanic areas, and the observed minimum and median diameters of the LECs decreases with increasing latitude. The observed minimum diameters of the LECs in the six planitiae within the northern lowlands suggest the roof depth of the LECs-forming layer has clear lateral variability, ranging between ~90 m in the Arcadia Planitia and ~280 m in the Isidis Planitia. The observed LECs are suggested to mainly form during the Amazonian, implying that the LEC-forming water-ice-bearing strata might be still present. The variation might reflect the comprehensive influence on the subsurface water-ice by the climate conditions and geologic events during the Amazonian period. The proposed subsurface stratigraphies in the six planitiae suggest that the total thickness of the LECs-related strata in the Chryse Planitia is the largest (~4.6 km) and in the Arcadia Planitia is the smallest (~1.6 km). There could be as much as ~3.5–16 million km^3 subsurface water stored in these strata, resulting in a ~24–110 m global equivalent layer (GEL) of water. Given that water is a fundamental ingredient to life, its migration from surface to subsurface shifts the focus of its exploration. Both Arcadia and Utopia Planitiae represent ideal candidates as locations where both shallow and deep subsurface water-ice might be abundant, they represent high-priority targets for future missions at mid-latitudes for biosignature searching and in-situ resource utilization.

1. Introduction

The barren and dry appearance of the current Martian surface bears the geological scars of a substantially wet past, in the form of dry riverbeds, delta plains, valley networks, etc. (e.g., Jons, 1985; Baker et al., 1991; Head et al., 1999; Fassett and Head, 2008; Di Achille and Hynek, 2010). The primordial Martian water volume produced by the catastrophic outgassing of the mantle could potentially be thousands of meters of global equivalent layer (GEL) (Elkins-Tanton, 2008). By measuring the current deuterium-to-hydrogen (D/H) ratio for the H_2O in the atmosphere, Villanueva et al. (2015) estimated that early Mars (4.5 billion years ago) had a GEL of water at least 137 m deep, covering 20% of the planet's surface. Zhu et al. (2022) proposed an early period of intense asteroid bombardment which might have accumulated enough water to create a > 300 m GEL of water, or even up to 1500 m GEL if the outgassing contribution from the molten mantle were to be added (Scheller et al., 2021). However, Carr and Head (2015) estimated only 34 m GEL of water currently lies in the Martian polar-layered deposits

* Corresponding author at: State Key Laboratory of Remote Sensing Science, Aerospace Information Research Institute, Chinese Academy of Sciences, Beijing 100101, China.
E-mail address: dikc@radi.ac.cn (K. Di).

https://doi.org/10.1016/j.icarus.2024.116100
Received 20 December 2023; Received in revised form 19 April 2024; Accepted 19 April 2024
Available online 25 April 2024

(PLDs) and the shallow ground ice (Plaut et al., 2007). Theoretical analysis (Clifford and Parker, 2001) and global subsurface water transport modelling (Grimm et al., 2017) show that there might be large quantities of widespread subsurface water-ice and/or liquid water stored in the deeper crust. This hypothesis is partially confirmed by the Mars Advanced Radar for Subsurface and Ionosphere Sounding (MARSIS) radar, which reveals that the water-ice locked up in the extensive deposits of Medusae Fossae Formation (MFF) at Mars's Equator is about 1.5 to 2.7 m GEL of water (Watters et al., 2024).

The substantial discrepancy between the (estimated) past and present water budget might be due largely to solar radiation (through photodissociation of water molecules), following the gradual loss of a strong magnetic shield (Villanueva et al., 2015; Stone et al., 2020). It is estimated that the integrated water loss to space is equivalent to at least 10 to 200 m GEL throughout Martian history (Lammer et al., 2003; Chaffin et al., 2014; Kurokawa et al., 2014; Villanueva et al., 2015; Jakosky et al., 2018; Alsaeed and Jakosky, 2019). Scheller et al. (2021) argued the atmospheric exodus process alone cannot explain modern aridity and they estimated that between 30% and 99% of the water was incorporated into the crust through hydration, i.e., a geologic entrapment in hydrated minerals. Riu et al. (2023) estimated the global water volume in present surficial hydrated silicates for deposits of 1 m in depth corresponds to only $\sim 10^{-4}$ m GEL, a rather low threshold that might indicate the hydrated silicates were not globally important water stores. However, the estimation should not be considered as a lower bound because it only counts spectrally detected hydrated silicates, which occupies a rather tiny fraction of the Martian surface areas that are free of dust cover and have significant exposures. The updated high-resolution map of Water Equivalent Hydrogen (WEH) in the Martian regolith shows several extremely high hydrogen regions at moderate latitudes and even near the equator, e.g., ~10 wt% WEH on the flanks of the Tharsis Montes, ~19 wt% at the Medusae Fossae Formation (MFF), ~23% at the Arabia Terra, ~40 wt% in the central part of Valles Marineris (Pathare et al., 2018; Wilson et al., 2018; Malakhov et al., 2022; Mitrofanov et al., 2022). Depending on the thickness of the hydrated minerals, these unusually high hydrogen abundances could amount to at least ~1 cm GEL as a lower bound. Mustard (2019) estimated the total water volume in the hydrated mineral over the 1 to 10 km Martian subsurface to have been about 15–1000 m GEL. Wernicke and Jakosky (2021) proposed the water stored within or needed to form hydrated minerals on Mars is 130–260 m GEL, and could be plausibly extended to 860 m GEL. In addition to being stored in hydrated minerals (Mustard, 2019; Riu et al., 2023; Scheller et al., 2021; Wernicke and Jakosky, 2021), in the subglacial salty lakes (Orosei et al., 2018; Lauro et al., 2021) and in the polar caps (Mitrofanov et al., 2002), water might also now be locked underground in aquifers (Gourronc et al., 2014; Mitrofanov et al., 2022), or in the shallow icy substrates (Byrne et al., 2009; Smith et al., 2009; Dundas et al., 2014, 2018, 2021; Stuurman et al., 2016; Piqueux et al., 2019).

Water is one of the key elements that influence both the geological evolution and potential habitability on the planet. Liquid water is not stable under modern atmosphere conditions on Mars, however, there could be undetected subsurface water/ice that exceeds the present observable water inventory (Kurokawa et al., 2014). To search for water beneath the Martian surface, craters represent unique probing tools. Direct observations of exposed shallow subsurface ice due to cratering have been already reported. Byrne et al. (2009) found geologically recent impacts in the mid-latitude poleward of about 40° excavated shallow (< 1 m in local sites) water ice, which might be a relic of the buried dusty snow layer deposited during high obliquity periods. Later observations confirmed the presence of high-purity shallow ice (Dundas et al., 2014; Dundas et al., 2018; Dundas et al., 2021), which extends down to a latitude of 35°N (Dundas et al., 2023).

Craters with special morphologies, e.g., ring-mold craters (Kress and Head, 2008), pedestal craters (Kadish et al., 2009), expanded craters (Viola et al., 2015), and terraced craters (Bramson et al., 2015), are thought to have formed by impacts into regions with shallow subsurface ice that might sublimate when exposed to the Martian atmosphere. They are usually formed through mechanisms that bear significant implications for the thickness and properties of the subsurface water-ice. For instance, Bramson et al. (2015) proposed the occurrence of a widespread, decameters-thick water-ice layer beneath the surface at the formation of the terraced craters in the Arcadia Planitia. Viola et al. (2015) estimated the minimum ice volume (140–360 km^3) sublimated during the formation of all the mapped expanded craters in the Arcadia Planitia corresponds to a global ice layer of ~1–2.5 mm, and there is still at least 6000 km^3 subsurface ice.

Craters with one or more layered ejecta deposits, known as layered ejecta craters (LECs), represent another distinct landform on the Martian surface. The LECs have been hypothesized to have formed by the interaction of the excavated material with the subsurface volatiles (volatile fluidization model) (e.g., Carr et al., 1977; Mouginis-Mark, 1979) and/or the atmosphere (atmospheric entrainment model) (e.g., Schultz and Gault, 1979; Barnouin-Jha and Schultz, 1998). In addition, the LECs, especially those with double-layered ejecta (DLE), were also proposed to be formed by impacting into a surface glacial ice layer that followed by landsliding of the ejecta off of the structurally uplifted rim (glacial substrate model) (Weiss and Head, 2013). Subsequent numerical simulations have produced LECs under Martian impact conditions with surface ice of 10–50 m thick (Alexander et al., 2023). The mostly accepted volatile fluidization model assumes the impact penetrates into a subsurface water-ice-rich stratum (usually >100 m deep), causing ejecta emplaced as a fluidized ground-hugging flow (e.g., Carr et al., 1977; Woronow, 1981; Barlow et al., 2001; Barlow and Perez, 2003; Barlow, 2005; Boyce and Mouginis-Mark, 2006; Senft and Stewart, 2008; Osinski et al., 2011; Kirchoff and Grimm, 2018). The LECs on the Martian surface have already been globally or regionally investigated with images of different resolutions (e.g., Demura and Kurita, 1998; Robbins and Hynek, 2012a; Barlow, 2017; Lagain et al., 2021; Gou et al., 2024) to analyze their spatial distribution and to infer subsurface properties. For instance, Kuzmin et al. (1988) inferred the depth to the top of an ice-rich layer where LECs are initially observed (hereinafter referred to as the roof depth) to be about 300–400 m at 30° latitude and decreases to about 50–100 m at 50°. Barlow et al. (2001) found the roof depth varies regionally within ±30° latitude and could be as shallow as 110 m in Solis and Thaumasia Planae. Reiss et al. (2005) estimated the subsurface ice table in the equatorial region of the Valles Marineris plateaus should be between ~75 m and ~ 260 m. Barlow and Perez (2003) confirmed the single layer ejecta (SLE) morphology is the dominant ejecta type within ±60° latitude (exceeding 70% of all ejecta morphologies for most of the area), and found the regional variations of the inferred subsurface volatiles correlate well with the possible locations of near-surface H_2O reservoirs detected by Mars Odyssey. Jones and Osinski (2015) developed a stratigraphic model to explain the observed trends after examining the regional variation in ejecta mobility, observed minimum diameter and their correlation for the SLE and DLE craters on Mars. Kirchoff and Grimm (2018) proposed tropical SLE craters formed throughout Amazonian, and their location near the radial ejecta craters implies strong lateral spatial heterogeneity of the relatively shallow subsurface ice.

The potential access to the rather shallow (generally <100 m) non-polar subsurface water-ice resources has been considered and assessed by the Mars Subsurface Water Ice Mapping (SWIM) project (Morgan et al., 2019; Morgan et al., 2021; Putzig et al., 2023); however, the distribution of the much deeper water-ice-bearing strata was beyond its original remit. This work centers on the further exploration of potential deep water-ice reservoirs, expanding on previous work, by focusing on LECs in northern Mars and introducing a stratigraphic analysis.

2. Study area

Although the Mars ocean idea is still in hot debate (Malin and Edgett,

1999), there is widespread evidence supporting the hypothesis that in its early history Mars featured large bodies of liquid water (either in the form of ocean or a series of large seas) in the northern lowlands, e.g., the Arabia Ocean (Contact 1) and Deuteronilus Ocean (Contact 2) (Head et al., 1999; Di Achille and Hynek, 2010; Citron et al., 2018; Saberi, 2020). This study thus focuses on the region that spans from the equator to 70° N (Fig. 1), which focuses on the six planitiae: Acidalia, Amazonia, Arcadia, Chryse, Isidis, and Utopia. The objective is to contribute to the planning of future Mars missions that target landing sites with greater insolation potential (Sun, 2022), and to complement the work of the SWIM project (Morgan et al., 2019; Morgan et al., 2021; Putzig et al., 2023),

3. Datasets and methods

3.1. Datasets

The datasets employed in this study include the Robbins and Hynek (2012a) database that has the most comprehensive Martian global crater ($\geq$ 1 km) survey, and the Lagain et al. (2021) database that further classified crater morphology. The ejecta morphologies, e.g., the number of layers and morphology of the LECs, were classified down to 1 km in diameter in both databases from the Thermal Emission Imaging System (THEMIS) mosaic (100 m/pixel) (Edwards et al., 2011). Therefore, the two crater databases are jointly used to ensure all identifiable LECs were used for our analyses: the latitudinal variation, density of the LECs, and the percentage of the LECs among all the craters, etc.

Our partner study in Gou et al. (2024) examined craters in the Chryse Planitia using the high-resolution Context Camera (CTX) mosaic (5 m/pixel) (Dickson et al., 2023), and found that measured diameters based upon THEMIS usually appears larger than that based upon CTX (Supplementary Fig. 1), with an average difference of about 9% (Supplementary Fig. 2). This average difference value is thus used for the uncertainty estimation when the analysis involves the size of the crater,

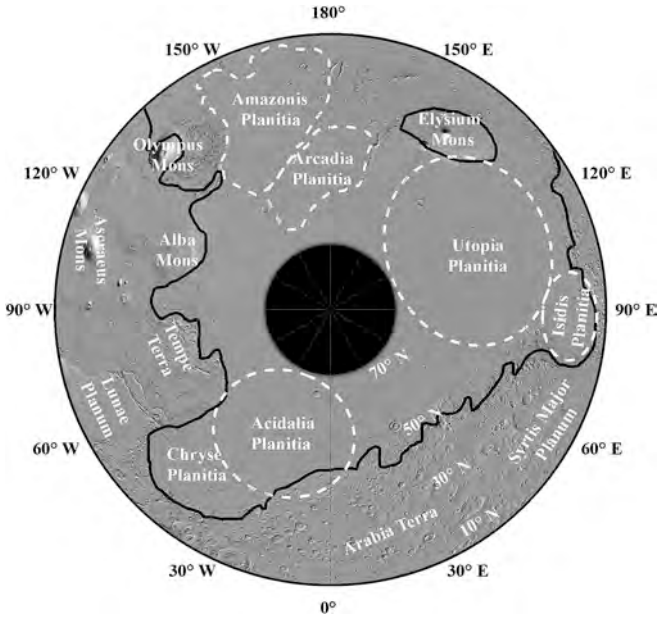

Fig. 1. The study area in northern Mars (0 to 70° N). The white dashed circles represent the approximate boundary of each planitia, and the black solid line outlines the potential paleo-shorelines of the Arabia Ocean, i.e., "Contact 1" in Head et al. (1999). The base map is the Mars Orbiter Laser Altimeter (MOLA) shaded relief (Smith et al., 2001). It should be noted that the shorelines of "Contact 1" do not follow an equipotential surface and there is extensive resurfacing north of the contact, and this has been used to argue against Mars once having an early ocean (Malin and Edgett, 1999).

e.g., determination of the excavation depth from the crater diameter.

In addition, there are craters that were missed (e.g., a crater with diameter $\geq$ 1 km was not identified), or mis-identified (e.g., a feature was mis-mapped as a crater), or mis-classified (e.g., a LEC was marked as a non-LEC) when using the THEMIS as a basemap (Supplementary Fig. 3). The craters in Chryse Planitia provide an example (Robbins and Hynek, 2012a; Lagain et al., 2021; Gou et al., 2024): there are suggested 23 missed craters, 91 misidentified or ghost craters, and 157 mis-classified craters. This evaluation shows that the mis-mapping and mis-classifying would result in an underestimation of the percentage of LECs (calculated from the number of LECs divided by the total number of craters), with an average of about 4% (Supplementary Table 1). Another factor that introduces uncertainty is the burial and/or erasure of the crater ejecta. Theoretically all craters start with some kind of ejecta after formation, and smaller craters are eroded and enlarged faster than the larger ones (Fassett and Thomson, 2014). Kirchoff et al. (2021) proposed the radial ejecta may be eroded faster than the layered ejecta if they form at roughly similar rates. When the layered ejecta (especially the small LECs) was partially or completely eroded away/buried, an incorrect identification would occur. The mis-identification would affect the classification (e.g., the pedestal crater) and number of LECs observed today and lead to the underestimation of the percentage of LECs. However, the effect of Mars crater degradation process on the identification of LECs is hard to estimate quantitatively at present, and the study is limited to the time frame, the Amazonian, when the effect is less. Nevertheless, when the analysis involves the percentage of LECs, the underestimation should be taken into account.

3.2. Methods

3.2.1. Determination of the excavation depth of a crater

It is hypothesized that the subsurface water-ice is most likely responsible for the formation of a majority of LECs (e.g., Carr et al., 1977; Woronow, 1981; Barlow et al., 2001; Barlow and Perez, 2003; Barlow, 2005; Boyce and Mouginis-Mark, 2006; Senft and Stewart, 2008; Osinski et al., 2011; Kirchoff and Grimm, 2018). Therefore, Therefore, we proceed with the assumption that the excavation depth of a LEC can be used to estimate the approximate boundary of the water-ice-rich layer that forms the LEC (i.e., an impact that penetrate into/through the depth would form a LEC). Melosh (1989) proposed the excavation depth (D_{exc}) of a crater to be about one-tenth of the diameter of the transient crater (D_t) (Eq. 1). For simple craters, D_t is approximately 0.84 times the crater's final rim-to-rim diameter (D_r) (Melosh, 1989). For complex craters, D_t is estimated by D_r using the relationship developed by Croft (1985):

$$D_{exc} \approx 0.1D_t \approx \begin{cases} 0.084D_r & D_r < D_{sc}\,(\text{simple crater}) \\ 0.1D_{sc}^{0.15}D_r^{0.85} & D_r \geq D_{sc}\ (\text{complex crater}) \end{cases} \quad (1)$$

where D_{sc} is the simple to complex crater transition diameter, which is ~6 km on average for Martian craters (Robbins and Hynek, 2012b).

For our procedure, the excavation depth estimated from the current observed smallest LEC in each planitia is considered to be the roof depth of the subsurface water-ice-rich layer where LECs are initially observed, and the excavation depth estimated from the current observed largest LEC is the maximum burial depth of the water-ice-rich layer that is conducive to the formation of LECs. Our LECs-related stratigraphy is then tentatively established based upon the excavation depth and the percentages of LECs among all the craters in the following section.

3.2.2. Construction of LECs-related strata

Each planitia features LECs with different diameters, and the excavation depth of each LEC can be estimated from the empirical eq. 1. Therefore, according to the percentages of LECs in different diameter range (e.g., 1–2 km, 2–3 km, 3–4 km) in each planitia, a preliminary stratigraphy related to the formation of LECs, and the relative,

qualitative abundance of the water-ice can be established (Fig. 2). The average water-ice abundance in the first stratum is unknown (LECs have not been observed yet), and its thickness is estimated from the excavation depth of the observed minimum diameter of the LECs; the second stratum has a relatively moderate water-ice abundance where LECs are initially observed: these account for the diameter range in which the LECs fraction is less than half (<50%) among all the impact craters, and its thickness is derived from the subtraction of the estimated minimum excavation depth for the first diameter range in which the proportion of LECs is >50% and the thickness of the first stratum; the third stratum has a relatively high water-ice abundance that causes the majority of LECs (≥50%) to form, where the thickness of this stratum is given by the subtraction of the estimated maximum excavation depth of the last diameter range in which the proportion of LECs is >50% and the thicknesses of the previous two strata; the fourth stratum also has a relatively moderate water-ice abundance that the proportion of LECs is <50%, and its thickness is the subtraction result of the estimated excavation depth of the largest LEC in the planitia and the thicknesses of the previous three strata; the fifth stratum is the base layer whose water-ice abundance and thickness cannot be estimated.

3.2.3. *Estimation of the possible (current) water volume in the LECs-related strata*

Formed early in Mars' history, the northern lowlands are repositories both of fluvial sediments and volcanic deposits. The planitiae within the lowlands are geologically relatively young, with large parts being mantled by the Hesperian-aged (>3.24 Ga) materials (Supplementary Fig. 4) (Hartmann, 2005; Tanaka et al., 2014). Grimm et al. (2017) found desiccation of the shallow water-ice to hundreds of meters GEL could occur just in hundreds of millions of years, depending on the climate conditions. Therefore, the burial depth and thickness of the subsurface shallow water-ice might have varied greatly in the six planitiae (especially those at low latitude). The model formation ages of the LECs suggest they were chiefly formed during the Amazonia period (<3.24 Ga) (Hartmann, 2005) (Supplementary Fig. 5) (Kirchoff and Grimm, 2018; Gou et al., 2024), indicating that the LEC-forming subsurface water-ice-bearing stratum may still be present throughout the last ~3 Ga.

An early simulation shows that the LECs' ejecta usually has a water abundance of 16–72% (Woronow, 1981). Subsequent simulations done by Senft and Stewart (2008) revealed the subsurface ice volume fraction should be at least 25% (≈23% water when the density difference (8%) between liquid water (i.e., 1 g/cm^3) and water-ice (i.e., 0.92 g/cm^3) is considered) for the observed effects, e.g., late-stage icy extrusions and increased level of fragmentation of the ejecta blanket. There is also plenty of evidences for fairly high ice contents at various (mostly shallow) depths, e.g., Durham et al. (2008) inferred the ground ice volume fraction of >35% (≈32% water) is possible on Mars. Both 23% and 32% are within the range of water abundance values reported by Woronow (1981). Therefore, assuming that the Martian subsurface has a constant water-ice abundance down to the maximum excavation depth of the largest LEC, the water volume in the LECs-related strata could be estimated for two separate ranges: a lower limit of 16%, and an upper limit of 72%.

Taken the percentage of LECs in a certain diameter range (it can be related to the thickness of a LEC-forming layer by eq. 1) as the area percentage that the layer has the LEC-forming region, we suggest the water volume in any LEC-forming layer can be estimated by the product of the area of the layer (i.e., the area of the planitia), the percentage of LECs in the layer, the thickness of the layer (determined from the diameter range), and the putative water abundance (i.e., 16% or 72%). Because we do not know what is in the upper or lower layers (Fig. 2), it follows that the minimum total possible (current) water volume in each planitia could be estimated by summing the water volume of each LEC-

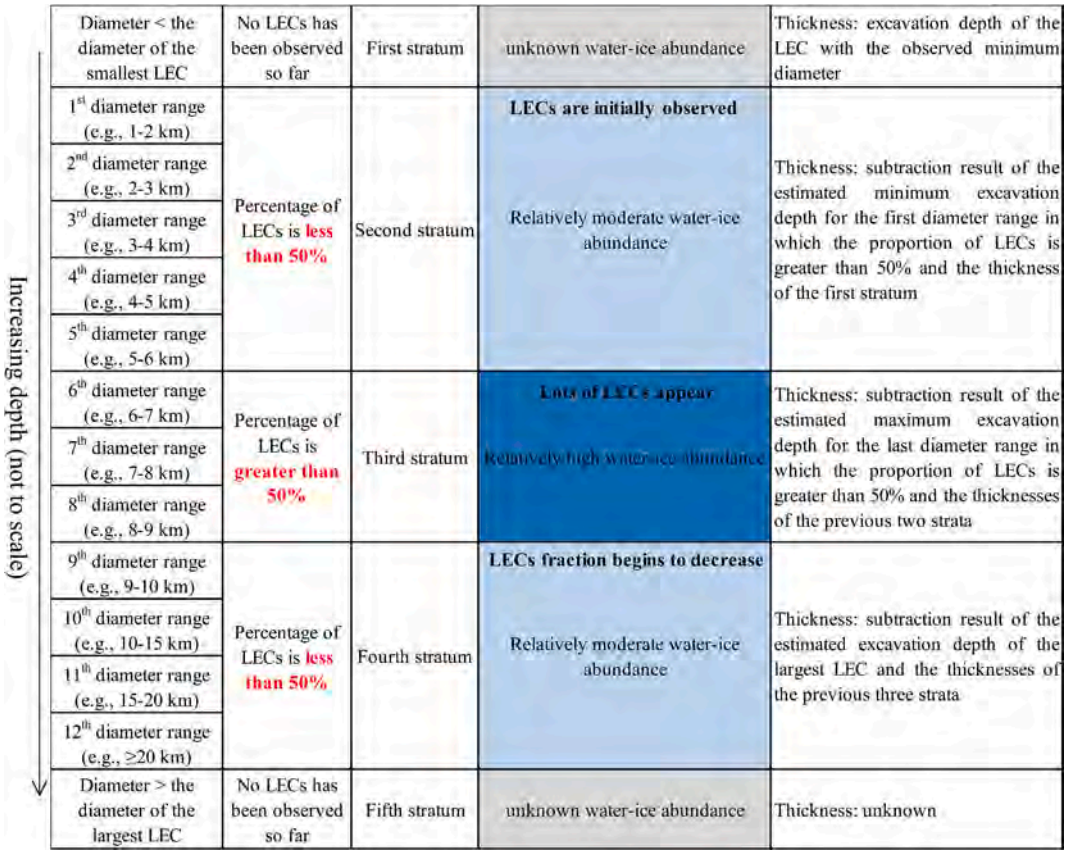

Fig. 2. Explanation of the construction of LECs-related stratigraphies.

forming layer (Fig. 3).

Since it seems implausible that a crater which excavated to 101 m into a water-ice-rich layer that begins at 100 m depth would have notable fluidized ejecta, as the excavated material has only a small fraction of the water-ice-rich material, therefore, it is difficult to determine the exact translation of the roof depth of the water-ice layer, especially because the abundance is expected to vary gradually. In addition, there are two possible scenarios for the estimated maximum burial depth of the water-ice-rich layer that is conducive to the formation of LECs. One case is that the estimated maximum burial depth is an underestimate, because the water-ice-containing layer may extend below this depth, but with a water fraction being too low to form LECs. Another case is that this depth is likely an overestimate, because excavating to just barely below the bottom of the water-rich layer would negligibly affect the average water fraction of the excavated material, and the largest LEC thus might be excavating fairly significantly into a layer with water content meaningfully less than the minimum value required for forming an LEC, to bring down the overall average water-ice content of the excavated material. Theoretical predictions like Grimm et al. (2017) or Clifford and Parker (2001) suggest a fairly sharp bottom to the water-ice-rich layer, which would lead to an abrupt drop in water-ice content rather than gradually dropping below the threshold, and the excavation depth would thus have to be some distance below that sharp cutoff before the effects are observed. No matter what the actual situation is, it will affect the estimated thickness of the LECs-related strata (but the direction of uncertainty is unknown). Based on the above explanation, it is thought the tentatively established stratigraphy in this study is being somewhat conservative. However, it is almost impossible to quantitatively analyze the uncertainty for the overestimation or underestimation. We thus proposed the uncertainty for both the thickness of the LECs-related strata and the estimated water volume are at least equivalent to the stated 9% uncertainty from crater diameter mismeasurement.

4. Results

4.1. General distribution characteristics of LECs

There are 9228 LECs in the databases used here (Robbins and Hynek, 2012a; Lagain et al., 2021) in the Martian northern region between 0 and 70°, with diameters ranging from 1.0 km to 111.1 km. A 2° × 2° grid mapping (1° × 1° and 5° × 5° mappings are shown in Supplementary Figs. 6 and 7) shows that there are generally few LECs in the volcanic areas, e.g., Olympus Mons, Ascraeus Mons, and the central of Amazonis Planitia, and there is (are) only one or two LEC(s) within many of the 2° × 2° grids (Fig. 4a and Supplementary Fig. 8). Both the observed minimum diameter (Fig. 4b) and the median of the diameter (Supplementary Fig. 9) of the LECs generally decrease with increasing latitude when all the LECs in the whole longitude domain (i.e. -180° to 180°) in each latitude range (e.g., 1°, 2°, and 5°) is considered. For example, the minimum and median diameters are ~3 km and ~ 7–8 km in the low latitudes of 0–30°, and are ~1 km and ~ 3–4 km in the high latitudes of 60–70°.

Among the six planitiae in the northern hemisphere, the Isidis Planitia has the highest crater density (0.0026/km^2, i.e., 2.6E-03/km^2 expressed in scientific notation) for diameter ≥ 1 km, and the Arcadia Planitia has the lowest (9.0E-04/km^2) (Table 1). However, the percentage of LECs shows an opposite trend, i.e., the Isidis Planitia has the lowest percentage of LECs (3.4%), and the Arcadia Planitia has the highest percentage (10.6%). Acidalia, Chryse, and Utopia Planitiae have similar crater densities and percentages of LECs, and Amazonis Planitia has slightly smaller values. The latitude-variation of the LECs in each planitia is shown in the Supplementary Figs. 10–15 and Supplementary Tables 2–7.

4.2. Excavation depths revealed by the LECs in each Planitia

The LEC with observed minimum diameter in each planitia varies from 1.1 km in the Arcadia Planitia to 3.3 km in the Isidis Planitia, corresponding to a roof depth of ~90 m and ~ 280 m, respectively (Table 1). The largest LECs in the six planitiae are different, e.g., the largest LEC in the Arcadia Planitia is 21.0 km, while in the Chryse

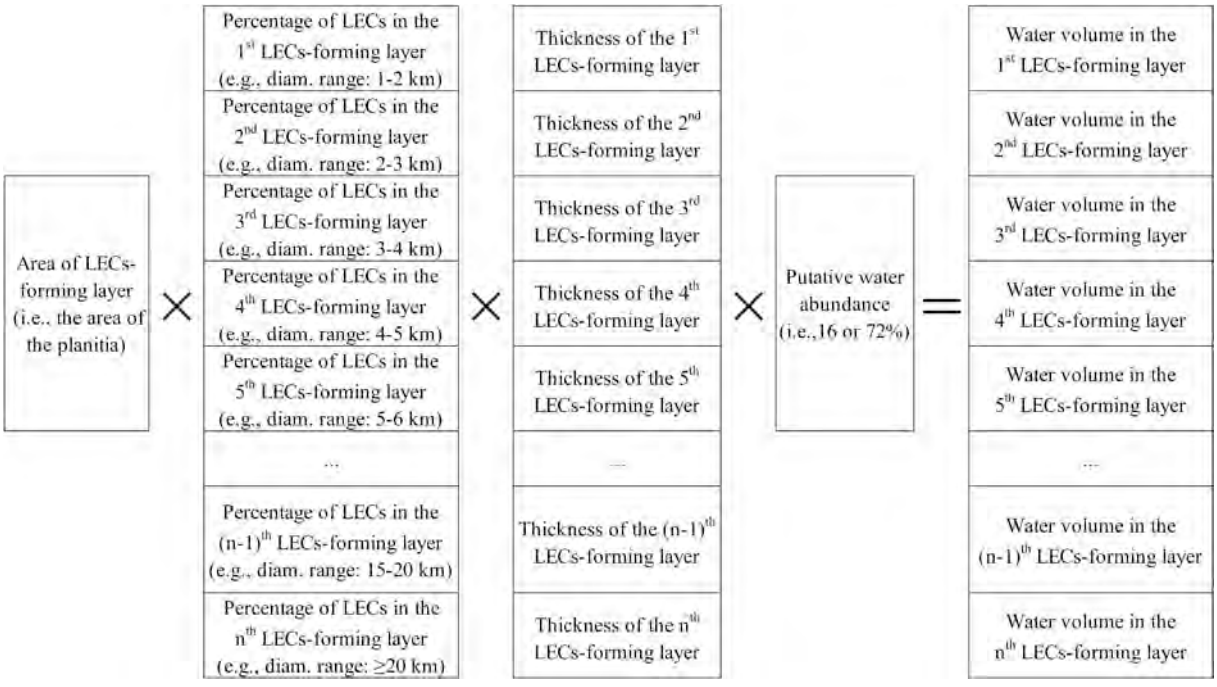

Fig. 3. Demonstration of estimation of water volume in each LECs-forming layer.

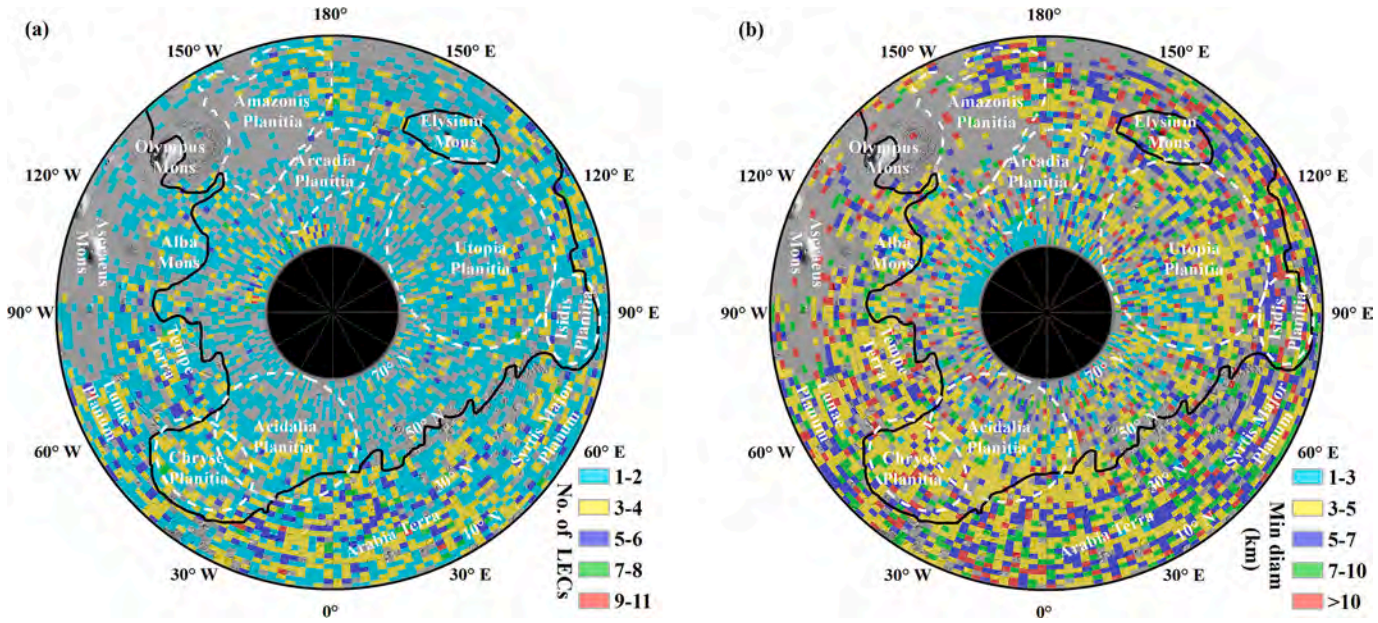

Fig. 4. (a) Number of the LECs within each 2° × 2°grid; (b) Observed minimum diameter of the LECs within each 2° × 2° grid. The base map is the MOLA shaded relief (Smith et al., 2001).

Table 1
LECs (diameter ≥ 1 km) in the Martian northern planitiae.

Planitia name		Acidalia[b]	Chryse	Utopia	Isidis	Amazonis	Arcadia
Number of craters		7399	3934	12,204	3012	3876	1655
Number of LECs		582	332	1043	101	245	175
Percentage of LECs		7.9%	8.4%	8.5%	3.4%	6.3%	10.6%
Area (km^2)[a]		3.9E+06	2.0E+06	7.5E+06	1.1E+06	3.7E+06	1.8E+06
Crater density (km^{-2})		1.9E-03	1.9E-03	1.6E-03	2.6E-03	1.0E-03	9.0E-04
LECs density (km^{-2})		1.5E-04	1.6E-04	1.4E-04	8.9E-05	6.6E-05	9.5E-05
LECs diam. range (km)	min.	1.5	1.5	1.5	3.3	1.7	1.1
	max.	55.7	67.3	46.3	35.7	59.5	21.0
Roof depth of the observed smallest LEC (m)		130	130	130	280	140	90
Excavation depth of the observed largest LEC (m)		3990	4680	3410	2730	4220	1740
Total thickness of the LECs-related strata (m)		3860	4550	3280	2450	4080	1650

[a] The area is calculated by the CraterTools (Kneissl et al., 2011), which is map-projection-independent and preserves the true area size.
[b] The overlapping region (Fig. 1) between Acidalia Planitia and Chryse Planitia is clipped for calculations related to the Acidalia Planitia (Supplementary Fig. 10), the area of Acidalia Planitia reported in the table is thus the area after clipping.

Planitia is 67.3 km (Table 1). Therefore, the maximum excavation depths of the LECs varies between ~1740 m and ~4680 m.

4.3. Stratigraphies of the LECs-related strata

The bar plots of the percentages of the LECs in different diameter ranges show that the LECs become the majority (over 50% among all the craters) from the diameter range of 4–5 km to the range of 9–10 km in the Acidalia Planitia (Fig. 5a), from the range of 4–5 km to 10–15 km in the Chryse Planitia (Fig. 5b), from the range of 3–4 km to 10–15 km in the Utopia Planitia (Fig. 5c), from the range of 7–8 km to 8–9 km in the Isidis Planitia (Fig. 5d). However, the percentage of LECs is >50% only in the diameter range of 8–9 km in the Amazonis Planitia (Fig. 5e), and the percentages in all the diameter ranges are below 50% in the Arcadia Planitia (Fig. 5f).

Following the methodology described in Section 3.2.2 (Fig. 2), a preliminary stratigraphy of the LECs-related strata can be established in each planitia (Fig. 6). The total thickness of the LECs-related strata (subtraction result of the maximum excavation depth and the roof depth) in the Chryse Planitia is the largest (~4.6 km), and in the Arcadia Planitia is the smallest (~1.7 km) (Table 1 and Fig. 6). The Utopia Planitia hosts the thickest stratum of relatively high average water-ice abundance (~1.1 km), where the majority (>50%) of the impacts penetrated into/through this stratum and formed LECs. The Amazonis Planitia hosts the thinnest stratum with relatively high average water-ice abundance (~80 m). Above the 90-m roof depth in the Arcadia Planitia, there appears to be a decameters-thick layer with water-ice, which might be responsible for the formation of terraced craters (Bramson et al., 2015). However, as a search for LECs <1 km in diameter has not been performed yet, the ability of the layer above the roof depth to produce them is unknown. Because the percentage of LECs in any diameter range does not exceed 50% (Fig. 5), according to the definition of the relatively high average water-ice abundance in the LECs-related stratum in Section 3.2.2, there appears to be no stratum with relatively high average water-ice abundance in the Arcadia Planitia (Fig. 6).

4.4. Water volume in the LECs-related strata

Estimation shows that the six planitiae might host at least ~3.5E+06 km^3 (~24 m GEL) subsurface water (likely in the form of water-ice deposits) in the LECs-related strata, and the volume could be as large as ~1.6E+07 km^3 (~110 m GEL) (Table 2). As the Utopia Planitia has the largest area (~7.5E+06 km^2) and a moderate thickness (~3.3 km) of LECs-related strata, it appears to host the largest subsurface water

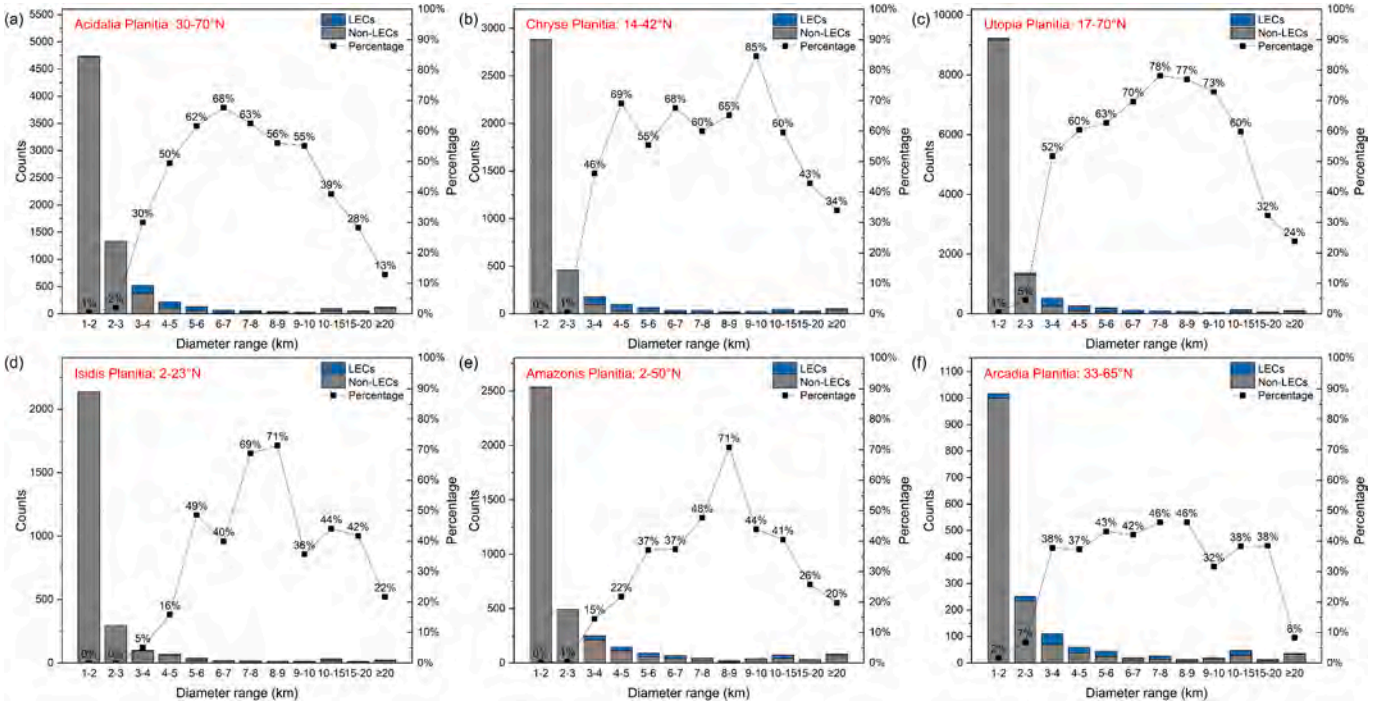

Fig. 5. Bar plots of the LECs and non-LECs in different diameter ranges in each planitia: (a) Acidalia Planitia; (b) Chryse Planitia; (c) Utopia Planitia; (d) Isidis Planitia; (e) Amazonis Planitia; (f) Arcadia Planitia. The blue and grey patches represent the number of LECs and non-LECs, respectively. The numbers associated with the points on the black solid line are the percentages of the LECs among all the craters, with an average underestimation of about 4% (see Section 3.1 for detail). The points above the horizontal black dashed line indicate the LECs become the majority among all the craters (percentage > 50%) in the corresponding diameter range. (For interpretation of the references to colour in this figure legend, the reader is referred to the web version of this article.)

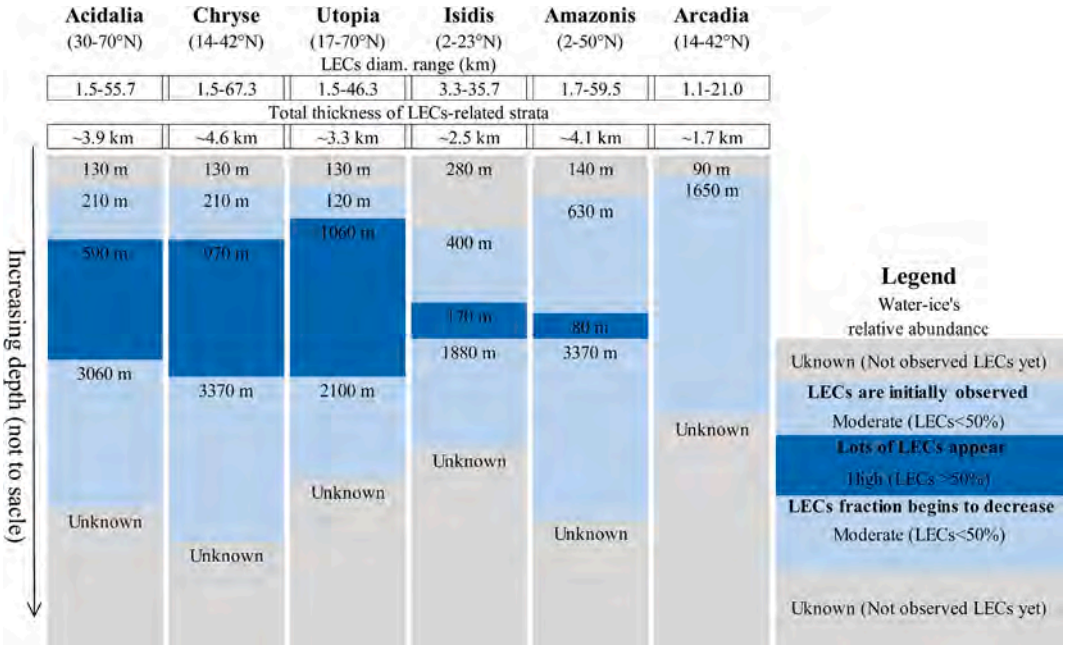

Fig. 6. Stratigraphies of the LECs-related strata in each planitia. The value (e.g., 130 m, 210 m, 590 m) in each stratum is the thickness. The average uncertainty for the estimated thickness of each stratum is at least 9% (see Section 3.2.3).

volume (~1.4E+06 km^3 /10 m GEL to ~6.5E+06 km^3 /45 m GEL). Although the total thickness of LECs-related strata (~2.5 km) in Isidis Planitia is larger than that (~1.7 km) in the Arcadia Planitia, its area (~1.1E+06 km^2) and percentage of LECs (3.4%) are smaller than those in the Arcadia Planitia, i.e., ~1.8E+06 km^2 and 10.6%, respectively. The Isidis Planitia hosts the smallest subsurface water volume.

5. Discussions

5.1. Implications of the roof depths

The observed minimum diameters of the LECs in each planitia suggest the roof depths of the LEC-forming water-ice-bearing layer have

Table 2
Estimated water volume in the LECs-related strata in each planitia.

Planitia name	Area (km^2)	Total thickness of LEC-related strata[b] (km)	Water volume[c] (km^3) (lower limit: 16%)	GEL of Water (m)	Water volume (km^3) (upper limit: 72%)	GEL of Water (m)
Acidalia[a]	3.9E+06	3.9	5.8E+05	4	2.6E+06	18
Chryse	2.0E+06	4.6	6.0E+05	4	2.7E+06	19
Utopia	7.5E+06	3.3	1.4E+06	10	6.5E+06	45
Isidis	1.1E+06	2.5	1.5E+05	1	6.7E+05	5
Amazonis	3.7E+06	4.1	5.9E+05	4	2.7E+06	18
Arcadia	1.8E+06	1.7	1.7E+05	1	7.5E+05	5
Total water volume (km^3)			3.5E+06	NA	1.6E+07	NA
Total GEL of water (m)			NA	24	NA	110

[a] The overlapping region (Fig. 1) between Acidalia Planitia and Chryse Planitia is clipped for calculations related to the Acidalia Planitia (Supplementary Fig. 10), the area of Acidalia Planitia reported in the table is thus the area after clipping.
[b] The average uncertainty for the estimated thickness is at least 9% (see Section 3.2.3).
[c] The water volume reported here is not estimated by directly multiplying the area, the total thickness of the LEC-related strata, the percentage of LECs, and the putative water abundance (i.e., 16% or 72%). A detailed description on the estimation can be found in Section 3.2.3. The uncertainty for the estimated volume is at least 9% (see Section 3.2.3).

evident lateral variability, varying between ~90 m in the Arcadia Planitia and ~280 m in the Isidis Planitia (Fig. 6). As a plain smoothed by the young Amazonian-aged lava flows that sourced from Elysium Mons and/or Olympus Mons, the Arcadia Planitia has undergone widespread glacial and periglacial activities after the emplacement of lava flooding, generating several viscous flow features (e.g., lobate debris aprons and lineated valley fill) that bear a striking resemblance to the landforms found on Earth in Antarctica (Hibbard et al., 2021). However, the prominent landform in the Isidis Planitia is the thumbprint terrain that consists of coalesced cones with central depressions or craters (Hiesinger et al., 2009). The formation scenarios of these cones, which are also found on other regions on Mars, are not very well understood and many terrestrial analogues have been proposed, e.g., pseudo-craters or rootless cones (Frey and Jarosewich, 1982), cinder cones (Meresse et al., 2008), mud volcanoes (Skinner and Mazzini, 2009), and pingos (Burr et al., 2005). Hiesinger et al. (2009) found the basal and central depression/crater diameters of these Amazonian-aged thumbprint cones in the Isidis Planitia are most consistent with cinder cones and pseudo-craters, suggesting they might be the products of the lava–ground ice interactions. Although might be rare, the basal melting of the young Amazonian glaciers in the Arcadia Planitia, due to climate cycles driven by orbital oscillations, is likely to replenish (Laskar et al., 2004; Butcher et al., 2017), while the volcanic activities in the Isidis Planitia would probably desiccate, the surface/subsurface water-ice on the same order as the thickness of an individual event, thus leading to the uplifting or lowering of the ground water-ice table. In addition to having undergone different geologic activities, the two planitiae are located at different latitudes (Fig. 1), with the Isidis being situated at much lower latitudes (2–23°N). Grimm et al. (2017) modelled the global desiccation of subsurface water on Mars, and the full evolutionary path implies hundreds of meters GEL water loss since the Hesperian is mainly due to obliquity. Lange et al. (2023) suggested the shallow subsurface water-ice beneath pole-facing slopes would not be at latitudes as low as previously thought in the ±30° latitude range. Therefore, the varying roof depths might indicate the comprehensive influence of the geologic activities and climate conditions on the subsurface water-ice. The roof depth estimation (~140 m) of the Amazonis Planitia might support this hypothesis. The Amazonis Planitia, also located between the Tharsis and Elysium volcanic provinces, has undergone alternating episodes of fluvial sediments and fluid lava flows (Campbell et al., 2008), resulting in an extremely smooth topography at several scale lengths (Fuller and Head, 2002). There are fewer LECs in the central region of the Amazonian-aged volcanic unit (25–35° N) (Supplementary Fig. 14), and the observed minimum diameter of the LECs in this region (3.0 km, corresponding to a roof depth of 250 m) is considerably larger than the one (1.8 km, roof depth being 150 m) in the mid-to-high latitudes (35–50° N), indicating the desiccation roles jointly played by the volcanic activities and climate conditions.

The Chryse, Acidalia, and Utopia Planitiae, all of which are part of the vast northern plains of Mars, share a similar roof depth (~130 m) of the LEC-forming water-ice-bearing layer (Fig. 6). The Chryse Planitia is thought to have contained a large lake or even an ocean that is associated with floods from surrounding giant outflow channel systems (e.g., Kasei Valles, Ares Vallis, Mawrth Vallis) during the Hesperian or early Amazonian periods (Tanaka, 1997). The largely flat Acidalia Planitia might also have contained a large number of floodwaters from the immediately adjacent Chryse Planitia in the south (Fig. 1). Following the disappearance of large bodies of water, mud volcanism became pervasive in this region during the early Amazonian period, forming widespread mounds over the large polygons (five to ten kilometers wide) (Oehler and Allen, 2010). The Utopia Planitia also hosts numerous giant polygons after the emplacement of the Vastitas Borealis Formation (VBF) unit. In situ observations of surface rocks and surveys on the subsurface structure suggest a origin in the occurrence of basin infilling deposition in a marine environment during the late Hesperian to Amazonian period (Li et al., 2022; Xiao et al., 2023). It thus seems that ancient water bodies, which might be important provenance of the subsurface water-ice table, were historically common in these three planitiae. A similar roof depth might suggest the existence of an underground water-ice-bearing layer that is favorable for the formation of LECs is widespread in these regions.

Because the roof depth discussed in this study is defined as the depth to the top of an ice-rich layer that is conducive to the formation of LECs, it should be noted that the absence of LECs above the roof depth does not necessarily indicate an absence of water-ice in the shallow subsurface (usually <100 m), e.g., a decameters-thick water-ice layer in Arcadia (Bramson et al., 2015). One reason is that since the crater databases used here only go down to 1 km (Robbins and Hynek, 2012a; Lagain et al., 2021), LECs with diameters less than the reported minimum ones have not been observed/catalogued yet. For example, previous works have already detected LECs with diameters less than or equal to 1 km (Reiss et al., 2005; Gou et al., 2024), corresponding to a roof depth of ~80 m or less. Future work (outside the scope of this publication) is needed to ensure smaller LECs are identified with high resolution images, such as the 5-m/pixel global CTX mosaic (Dickson et al., 2023), to better understand the variation and implication of the roof depths. Another possible reason is that the average abundance of the water-ice in the stratum above the roof depth is less than that required for the ejecta to be fluidized (under the assumption that all the LECs have already been identified). Laskar et al. (2004) derived Mars' obliquity history over the past 20 Myr and found that it oscillated between ~15–35° during the last 4.5 Myr following a higher obliquity (≥35–40°, average: ~36°) period. Glacial activities at times of high obliquity would cause the migration of water-ice from the polar ice caps to the mid-latitude ice

sheets (Laskar et al., 2004; Head et al., 2006), which may be later buried by crater ejecta and/or volcanic ash. For example, the scalloped depressions and polygonal terrain in the Utopia Planitia suggest the presence of a substantial volume of near-surface ice, which is above the roof depth and is likely a mantling layer that was deposited during the high obliquity period. Although clean shallow ice has been exposed by new impacts at the mid-latitudes (Dundas et al., 2014; Dundas et al., 2018; Dundas et al., 2021; Dundas et al., 2023) and has been observed directly by the Phoenix lander at high latitude (Smith et al., 2009), it is known that only when the average subsurface water abundance exceeds a certain threshold (e.g., 16%–72%) can the ejecta be sufficiently fluidized (Woronow, 1981; Durham et al., 2008; Senft and Stewart, 2008). Furthermore, the work done by Alexander et al. (2023) indicate a surface ice layer of 10 m may result in a LEC (depending on crater size). Therefore, the missing LECs above the roof depth might be a result of the very spatially and temporally heterogeneous water-ice abundance, which leads to a relatively low average water-ice abundance that cannot fluidize the ejecta. Other possible reasons include small impacts do not have enough energy to produce LECs for some unknown reasons, or that small LECs are more easily modified/mantled and become unrecognizable. Poleward of about 45° latitude, it has been suggested ground ice should be stable at shallow depths throughout plausible obliquity variations (e.g., Mellon and Jakosky, 1993; Mellon and Sizemore, 2022). It is thus expected that every small crater up there would be a LEC, but they might be too modified to recognize.

5.2. Implications of the LECs-related strata

The estimated total thickness of the LECs-related strata in the Acidalia planitia (~ 3860 m) is comparable to that of subsurface stratification model proposed by Costard and Kargel (1995) (~940–1000 m massive ice layer + >2500 m less ice-rich layer), indicating the constructed strata in each planitia may represent a useful guide for current and future radar surveys. For instance, the MARSIS could potentially penetrate the Martian surface down to about 5 km (Picardi et al., 2004), which is beyond the estimated maximum thickness of the LECs-related strata in the six planitiae (i.e., ~4550 m in the Chryse). A water ice deposit of 80–170 m thick in the western Utopia Planitia has already been detected (Stuurman et al., 2016) by the SHAllow RADar (SHARAD) that is able to penetrate up to half-a-kilometer deep (Seu et al., 2007). Therefore, although the MARSIS team has studied the northern plains in the early days (e.g., Mouginot et al., 2012), a re-analysis of the spatially coarse, but deep sounding complete MARSIS dataset, similar to what has been done to reveal the ice-rich layered deposits in the Martian equatorial Medusae Fossae Formation (MFF) (Watters et al., 2024), is needed to test the findings reported in this study. However, the MARSIS data may be limited by the instrument's vertical and horizontal resolution, or by the lack of dielectric contrast between different LECs-related strata (i.e., interfaces are not sharp enough), or by the attenuation of the radar signal. The proposed International Mars Ice Mapper (I-MIM) mission has already aimed to map the location, depth, spatial extent, abundance, and purity of the near-surface (top 5–10 m) water ice (Davis and Haltigin, 2021). Ideally, a novel dedicated radar instrument optimized with high-resolution capabilities to map the relatively deep subsurface water-ice should be proposed for future orbital missions. However, this sort of radar experiment may simply not be practical if the Martian crust is too attenuating.

5.3. Implications of the estimated water volume

LECs are found across the entire Martian surface, e.g., Barlow (2005), Robbins and Hynek (2012a), and Lagain et al. (2021). The area of the six planitiae investigated in this study covers only ~14% of the area of Mars, which seems to suggest a rather surprisingly large subsurface water reservoir when the estimated water volumes in the six planitiae (Table 2) are scaled to the whole surface of Mars and assuming all LECs are produced by tapping subsurface ice, i.e., ~170 m GEL under the 16% water abundance assumption, and ~780 m GEL in the 72% case. Both the low-end of ~170 m GEL and the high-end of ~780 m GEL are in the range of the (primordial) water inventory estimates inferred from different approaches (Carr and Head, 2003; Lunine et al., 2003; Elkins-Tanton, 2008; Scheller et al., 2021), indicating enormous amounts of water might have been cycled through the surface hydrological activities (e.g., fluvial processes that form valley networks), and then largely frozen underground. The spatial distribution, temporal variation, abundance heterogeneity, and paleoclimate implications of the subsurface water-ice in the LECs-related strata (e.g., Kirchoff et al., 2021; Gou et al., 2024) should thus be further studied to solve problems like why not all craters in the optimal size range are always LECs and the latitude-variation of the subsurface water-ice.

As water represents an indispensable ingredient for supporting life, its plausible sequestering might have changed the potential locations for the preservation/emergence of ancient life to retreat from the surface to the subsurface (meters to kilometers below the surface). The much deeper water-ice is a good place for shielding the harsh Martian environment for the preservation/emergence of life. On the other hand, shallow water-ice is an important easily accessible resource for in-situ resource utilization (ISRU) (e.g., life support and fuel production). Therefore, the regions with abundant both shallow and deep subsurface water-ice might represent ideal places for ISRU and biosignature searching for future Mars missions (i.e., gain two advantages in a single mission), especially the manned ones that are able to complete tasks with sophisticated payloads, such as drilling a core.

Both the United States of America (USA) and China have planned Mars sample return (MSR) missions, which aim to deliver samples to Earth around the year 2030 (Cataldo et al., 2022; Sun, 2022). The USA MSR mission will recover sample tubes encapsulated by the Perseverance rover that landed on Mars in 2021 to study Mars' biological evolution (Cataldo et al., 2022). However, the landing site of China's MSR mission has not been formalized as yet. Among the six planitiae, the SWIM project suggested the Arcadia and Utopia Planitiae as potentially favorable regions for finding accessible rather shallow (generally <10 m) subsurface water ice (Supplementary Fig. 16) (Morgan et al., 2021).

This study reveals that both the Arcadia and Utopia Planitiae also are quite favorable to the formation of LECs (the percentage of LECs among all craters are 10.6% and 8.5%, respectively, Table 1), and the roof depth of the LEC-forming strata are the top two shallowest (~90 m and ~ 130 m, respectively, Fig. 6) among the six planitiae. Simulation reveals that the impact-generated hydrothermal systems could keep active for 10^4–10^7 years, and are capable of forming clay minerals, e.g., phyllosilicates (Schwenzer and Kring, 2009). The presence of subsurface water-ice in the LECs-related strata and the clay minerals have great astrobiological significance, and the evidence of subsurface life (if any) could be exhumed during crater formation and retained within the ejecta deposits (Cockell and Barlow, 2002). It is thus proposed that the Arcadia and Utopia Planitiae should be considered as high-priority regions at mid-latitudes for future Mars exploration missions, for example, MSR missions aimed at (ancient) life searching and human-landing missions for ISRU. However, special attention must be paid for planetary protection for any potential future robotic or manned missions to Mars to avoid biological contamination (Rummel et al., 2014).

6. Conclusions

The analysis of the distribution and implications of LECs in northern Mars, especially in the six planitiae, i.e., Acidalia, Chryse, Utopia, Isidis, Amazonis, and Arcadia, was the focus of this study. The LECs were found to show a regional and latitudinal variation. There are generally few LECs in volcanic areas, and the current observed minimum and median diameters of the LECs decrease with increasing latitude, e.g., the observed minimum and median diameters are ~3 km and ~7–8 km in the low latitudes of 0–30°, and are ~1 km and ~3–4 km in the high

latitudes of 60–70°. The current observed minimum diameters of the LECs in each planitia suggest the roof depths of the primary LEC-forming stratum have lateral variability, varying between ~90 m in Arcadia Planitia and ~280 m in Isidis Planitia. The variation might reflect the joint effects of the climate conditions and the geologic activities during the Amazonian period on the subsurface water-ice.

The constructed stratigraphies in the six planitiae reveal that the total thickness of the LECs-related strata in the Chryse Planitia to be the largest (~4.6 km) against the smallest in the Arcadia Planitia (~1.7 km). The six planitiae might host at least ~3.5E+06 km^3/~24 m GEL subsurface water in the LECs-related strata, with the Utopia Planitia bearing the largest volume (~1.4E+06 km^3/~10 m GEL) and the Isidis Planitia storing the smallest (~1.5E+05 km^3/~1 m GEL). The Arcadia and Utopia Planitiae are proposed as high-priority regions at mid-latitudes for future missions, due to their likely abundant both shallow and deep subsurface water-ice for ISRU and biosignature searching potential.

The next step will be to carry out a global-scale re-mapping of the LECs with the recently released high-resolution CTX mosaic (Dickson et al., 2023). The re-mapping will undoubtedly better constrain the water volume stored in the LECs-related strata, thus enhancing our understanding of the evolution of water on Mars and potentially aiding the selection of the optimal landing areas for the upcoming Mars exploration programs, e.g., China's MSR mission (Sun, 2022).

CRediT authorship contribution statement

Zongyu Yue: Writing – review & editing, Writing – original draft, Methodology, Investigation, Funding acquisition, Formal analysis, Data curation, Conceptualization. **Kaichang Di:** Writing – review & editing, Writing – original draft, Validation, Supervision, Project administration, Methodology, Investigation, Funding acquisition, Formal analysis, Data curation, Conceptualization. **Patrick C. Pinet:** Writing – review & editing, Writing – original draft, Validation, Methodology, Investigation, Formal analysis, Data curation. **Roberto Bugiolacchi:** Writing – review & editing, Writing – original draft, Methodology, Investigation, Funding acquisition, Formal analysis, Data curation. **Shengli Niu:** Writing – review & editing, Writing – original draft, Methodology, Investigation, Funding acquisition. **Zhanchuan Cai:** Writing – review & editing, Writing – original draft, Methodology, Investigation, Formal analysis, Data curation. **Shuanggen Jin:** Writing – review & editing, Writing – original draft, Methodology, Investigation, Funding acquisition, Formal analysis.

Declaration of competing interest

The authors declare that they have no known competing financial interests or personal relationships that could have appeared to influence the work reported in this article.

Data availability

The data used in the study are from public Mars crater database

Acknowledgements

This research is supported by the National Key Research and Development Program of China (grant No. 2021YFA0716100), Strategic Priority Research Program of the Chinese Academy of Sciences (grant No. XDB41000000), National Natural Science Foundation of China (grant Nos. 42172265 and 42241111), Macao Young Scholars Program (grant No. AM201902), and the Key Research Program of the Institute of Geology and Geophysics, Chinese Academy of Sciences (grant No. IGGCAS-202204). The authors would like to thank Prof. Michelle Kirchoff and an anonymous reviewer for the meticulous, constructive and insightful review that improved the quality of the manuscript substantially, and Dr. Brandon Johnson for the effective editorial handling.

Appendix A. Supplementary data

Supplementary data to this article can be found online at https://doi.org/10.1016/j.icarus.2024.116100.

References

Alexander, A.M., Grimm, R.E., Kirchoff, M.R., 2023. Formation of layered-ejecta craters during Martian glaciations: insights from numerical modeling. In: 54th Lunar and Planetary Science Conference. The Woodlands, Texas and virtually, pp. 2795.
Alsaeed, N.R., Jakosky, B.M., 2019. Mars water and D/H evolution from 3.3 Ga to present. J. Geophys. Res. Planets. 124 (12), 3344–3353.
Baker, V.R., Strom, R.G., Gulick, V.C., Kargel, J.S., Komatsu, G., Kale, V.S., 1991. Ancient oceans, ice sheets and the hydrological cycle on Mars. Nature 352 (6336), 589–594.
Barlow, N.G., 2005. A review of Martian impact crater ejecta structures and their implications for target properties. In: Kenkmann, T., Hörz, F., Deutsch, A. (Eds.), Large Meteorite Impacts III, Geological Society of America Special Paper, 384, pp. 433–442.
Barlow, N.G., 2017. Revision of the "catalog of large Martian impact craters" and comparison to other Martian crater databases. In: 48th Lunar and Planetary Science Conference. The Woodlands, Texas, p. 1562.
Barlow, N.G., Perez, C.B., 2003. Martian impact crater ejecta morphologies as indicators of the distribution of subsurface volatiles. J. Geophys. Res. Planets. 108 (E8), 5085.
Barlow, N.G., Koroshetz, J., Dohm, J.M., 2001. Variations in the onset diameter for Martian layered ejecta morphologies and their implications for subsurface volatile reservoirs. Geophys. Res. Lett. 28 (16), 3095–3098.
Barnouin-Jha, O.S., Schultz, P.H., 1998. Lobateness of impact ejecta deposits from atmospheric interactions. J. Geophys. Res. Planets. 103 (E11), 25739–25756.
Boyce, J.M., Mouginis-Mark, P.J., 2006. Martian craters viewed by the thermal emission imaging system instrument: double-layered ejecta craters. J. Geophys. Res. Planets. 111 (E10), E10005.
Bramson, A.M., Byrne, S., Putzig, N.E., Sutton, S., Plaut, J.J., Brothers, T.C., Holt, J.W., 2015. Widespread excess ice in Arcadia Planitia, Mars. Geophys. Res. Lett. 42 (16), 6566–6574.
Burr, D.M., Soare, R.J., Tseung, Wan Bun, J.-M., Emery, J.P., 2005. Young (late Amazonian), near-surface, ground ice features near the equator, Athabasca Valles, Mars. Icarus 178 (1), 56–73.
Butcher, F.E.G., Balme, M.R., Gallagher, C., Arnold, N.S., Conway, S.J., Hagermann, A., Lewis, S.R., 2017. Recent basal melting of a mid-latitude glacier on Mars. J. Geophys. Res. Planets. 122 (12), 2445–2468.
Byrne, S., Dundas, C.M., Kennedy, M.R., Mellon, M.T., McEwen, A.S., Cull, S.C., Daubar, I.J., Shean, D.E., Seelos, K.D., Murchie, S.L., Cantor, B.A., Arvidson, R.E., Edgett, K.S., Reufer, A., Thomas, N., Harrison, T.N., Posiolova, L.V., Seelos, F.P., 2009. Distribution of mid-latitude ground ice on Mars from new impact craters. Science 325 (5948), 1674–1676.
Campbell, B., Carter, L., Phillips, R., Plaut, J., Putzig, N., Safaeinili, A., Seu, R., Biccari, D., Egan, A., Orosei, R., 2008. SHARAD radar sounding of the Vastitas Borealis Formation in Amazonis Planitia. J. Geophys. Res. Planets. 113 (E12), E12010.
Carr, M.H., Head, J.W., 2003. Oceans on Mars: an assessment of the observational evidence and possible fate. J. Geophys. Res. Planets. 108 (E5), 5042.
Carr, M.H., Head, J.W., 2015. Martian surface/near-surface water inventory: sources, sinks, and changes with time. Geophys. Res. Lett. 42 (3), 726–732.
Carr, M.H., Crumpler, L.S., Cutts, J.A., Greeley, R., Guest, J.E., Masursky, H., 1977. Martian impact craters and emplacement of ejecta by surface flow. J. Geophys. Res. 82 (28), 4055–4065.
Cataldo, G., Childs, B., Corliss, J., Feehan, B., Gage, P., Lin, J., Mukherjee, S., Neuman, M., Pellerano, F., Sarli, B., Szalai, C., Teeney, L., Kam, J.V., White, T., Yew, C., Zumwalt, C., 2022. Mars sample return – An overview of the capture, containment and return system. In: 73rd International Astronautical Congress. Paris, France pp. IAC-22-A3.3A.10.
Chaffin, M.S., Chaufray, J.-Y., Stewart, I., Montmessin, F., Schneider, N.M., Bertaux, J.-L., 2014. Unexpected variability of Martian hydrogen escape. Geophys. Res. Lett. 41 (2), 314–320.
Citron, R.I., Manga, M., Hemingway, D.J., 2018. Timing of oceans on Mars from shoreline deformation. Nature 555 (7698), 643–646.
Clifford, S.M., Parker, T.J., 2001. The evolution of the Martian hydrosphere: implications for the fate of a primordial ocean and the current state of the northern plains. Icarus 154 (1), 40–79.
Cockell, C.S., Barlow, N.G., 2002. Impact excavation and the search for subsurface life on Mars. Icarus 155 (2), 340–349.
Costard, F.M., Kargel, J.S., 1995. Outwash plains and thermokarst on Mars. Icarus 114 (1), 93–112.
Croft, S.K., 1985. The scaling of complex craters. J. Geophys. Res. Solid Earth 90 (S02), C828–C842.
Davis, R., Haltigin, T., 2021. International Mars ice mapper mission: the first human exploration reconnaissance mission to Mars. In: 52nd Lunar and Planetary Science Conference. Held Virtually, pp. 2614.
Demura, H., Kurita, K., 1998. A shallow volatile layer at Chryse Planitia, Mars. Earth Planets Space 50 (5), 423–429.

Di Achille, G., Hynek, B.M., 2010. Ancient ocean on Mars supported by global distribution of deltas and valleys. Nat. Geosci. 3 (7), 459–463.
Dickson, J.L., Ehlmann, B.L., Kerber, L.H., Fassett, C.I., 2023. Release of the global CTX mosaic of Mars: an experiment in information-preserving image data processing. In: 54th Lunar and Planetary Science Conference. The Woodlands, Texas and Virtually, pp. 2353.
Dundas, C.M., Byrne, S., McEwen, A.S., Mellon, M.T., Kennedy, M.R., Daubar, I.J., Saper, L., 2014. HiRISE observations of new impact craters exposing Martian ground ice. J. Geophys. Res. Planets. 119 (1), 109–127.
Dundas, C.M., Bramson, A.M., Ojha, L., Wray, J.J., Mellon, M.T., Byrne, S., McEwen, A. S., Putzig, N.E., Viola, D., Sutton, S., Clark, E., Holt, J.W., 2018. Exposed subsurface ice sheets in the Martian mid-latitudes. Science 359 (6372), 199–201.
Dundas, C.M., Mellon, M.T., Conway, S.J., Daubar, I.J., Williams, K.E., Ojha, L., Wray, J. J., Bramson, A.M., Byrne, S., McEwen, A.S., Posiolova, L.V., Speth, G., Viola, D., Landis, M.E., Morgan, G.A., Pathare, A.V., 2021. Widespread exposures of extensive clean shallow ice in the midlatitudes of Mars. J. Geophys. Res. Planets. 126 (3), e2020JE006617.
Dundas, C.M., Mellon, M.T., Posiolova, L.V., Miljković, K., Collins, G.S., Tornabene, L.L., Rangarajan, V.G., Golombek, M.P., Warner, N.H., Daubar, I.J., Byrne, S., McEwen, A. S., Seelos, K.D., Viola, D., Bramson, A.M., Speth, G., 2023. A large new crater exposes the limits of water ice on Mars. Geophys. Res. Lett. 50 (2), e2022GL100747.
Durham, W.B., Pathare, A.V., Stern, L.A., 2008. The brittle-to-ductile transition of icy materials on Mars. In: 39th Lunar and Planetary Science Conference. League City, Texas, pp. 2315.
Edwards, C., Nowicki, K., Christensen, P., Hill, J., Gorelick, N., Murray, K., 2011. Mosaicking of global planetary image datasets: 1. Techniques and data processing for thermal emission imaging system (THEMIS) multi-spectral data. J. Geophys. Res. 116 (E10), E10008.
Elkins-Tanton, L.T., 2008. Linked magma ocean solidification and atmospheric growth for Earth and Mars. Earth Planet. Sci. Lett. 271 (1), 181–191.
Fassett, C.I., Head, J.W., 2008. Valley network-fed, open-basin lakes on Mars: distribution and implications for Noachian surface and subsurface hydrology. Icarus 198 (1), 37–56.
Fassett, C.I., Thomson, B.J., 2014. Crater degradation on the lunar maria: topographic diffusion and the rate of erosion on the Moon. J. Geophys. Res. Planets. 119 (10), 2255–2271.
Frey, H., Jarosewich, M., 1982. Subkilometer Martian volcanoes: properties and possible terrestrial analogs. J. Geophys. Res. Solid Earth 87 (B12), 9867–9879.
Fuller, E.R., Head, J.W. III., 2002. Amazonis Planitia: the role of geologically recent volcanism and sedimentation in the formation of the smoothest plains on Mars. J. Geophys. Res. Planets. 107 (E10), 5081.
Gou, S., Yue, Z., Di, K., Bugiolacchi, R., Niu, S., Cai, Z., Liu, B., Jin, S., 2024. Paleoenvironment implications of layered ejecta craters in the Chryse Planitia, Mars. Icarus 410, 115918.
Gourronc, M., Bourgeois, O., Mège, D., Pochat, S., Bultel, B., Massé, M., Le Deit, L., Le Mouélic, S., Mercier, D., 2014. One million cubic kilometers of fossil ice in Valles Marineris: relicts of a 3.5Gy old glacial landsystem along the Martian equator. Geomorphology 204, 235–255.
Grimm, R.E., Harrison, K.P., Stillman, D.E., Kirchoff, M.R., 2017. On the secular retention of ground water and ice on Mars. J. Geophys. Res. Planets. 122 (1), 94–109.
Hartmann, W.K., 2005. Martian cratering 8: Isochron refinement and the chronology of Mars. Icarus 174 (2), 294–320.
Head, J.W., Hiesinger, H., Ivanov, M.A., Kreslavsky, M.A., Pratt, S., Thomson, B.J., 1999. Possible ancient oceans on Mars: evidence from Mars orbiter laser altimeter data. Science 286 (5447), 2134–2137.
Head, J.W., Nahm, A.L., Marchant, D.R., Neukum, G., 2006. Modification of the dichotomy boundary on Mars by Amazonian mid-latitude regional glaciation. Geophys. Res. Lett. 33 (8), L08S03.
Hibbard, S.M., Williams, N.R., Golombek, M.P., Osinski, G.R., Godin, E., 2021. Evidence for widespread glaciation in Arcadia Planitia, Mars. Icarus 359, 114298.
Hiesinger, H., Rohkamp, D., Sturm, S., Thiessen, F., Reiss, D., 2009. Geology, ages, morphology, and morphometry of thumbprint terrain in Isidis Planitia, Mars. In: 40th Lunar and Planetary Science Conference. the Woodlands, Texas, pp. 1953.
Jakosky, B.M., Brain, D., Chaffin, M., Curry, S., Deighan, J., Grebowsky, J., Halekas, J., Leblanc, F., Lillis, R., Luhmann, J.G., Andersson, L., Andre, N., Andrews, D., Baird, D., Baker, D., Bell, J., Benna, M., Bhattacharyya, D., Bougher, S., Bowers, C., Chamberlin, P., Chaufray, J.Y., Clarke, J., Collinson, G., Combi, M., Connerney, J., Connour, K., Correira, J., Crabb, K., Crary, F., Cravens, T., Crismani, M., Delory, G., Dewey, R., DiBraccio, G., Dong, C., Dong, Y., Dunn, P., Egan, H., Elrod, M., England, S., Eparvier, F., Ergun, R., Eriksson, A., Esman, T., Espley, J., Evans, S., Fallows, K., Fang, X., Fillingim, M., Flynn, C., Fogle, A., Fowler, C., Fox, J., Fujimoto, M., Garnier, P., Girazian, Z., Groeller, H., Gruesbeck, J., Hamil, O., Hanley, K.G., Hara, T., Harada, Y., Hermann, J., Holmberg, M., Holsclaw, G., Houston, S., Inui, S., Jain, S., Jolitz, R., Kotova, A., Kuroda, T., Larson, D., Lee, Y., Lee, C., Lefevre, F., Lentz, C., Lo, D., Lugo, R., Ma, Y.J., Mahaffy, P., Marquette, M.L., Matsumoto, Y., Mayyasi, M., Mazelle, C., McClintock, W., McFadden, J., Medvedev, A., Mendillo, M., Meziane, K., Milby, Z., Mitchell, D., Modolo, R., Montmessin, F., Nagy, A., Nakagawa, H., Narvaez, C., Olsen, K., Pawlowski, D., Peterson, W., Rahmati, A., Roeten, K., Romanelli, N., Ruhunusiri, S., Russell, C., Sakai, S., Schneider, N., Seki, K., Sharrar, R., Shaver, S., Siskind, D.E., Slipski, M., Soobiah, Y., Steckiewicz, M., Stevens, M.H., Stewart, I., Stiepen, A., Stone, S., Tenishev, V., Terada, N., Terada, K., Thiemann, E., Tolson, R., Toth, G., Trovato, J., Vogt, M., Weber, T., Withers, P., Xu, S., Yelle, R., Yiğit, E., Zurek, R., 2018. Loss of the Martian atmosphere to space: present-day loss rates determined from MAVEN observations and integrated loss through time. Icarus 315, 146–157.
Jones, E., Osinski, G.R., 2015. Using martian single and double layered ejecta craters to probe subsurface stratigraphy. Icarus 247, 260–278.
Jons, H.-P., 1985. Late sedimentation and late sediments in the northern lowlands on Mars. In: 16th Lunar and Planetary Science Conference. Houston, Texas, pp. 414–415.
Kadish, S.J., Barlow, N.G., Head, J.W., 2009. Latitude dependence of Martian pedestal craters: evidence for a sublimation-driven formation mechanism. J. Geophys. Res. Planets. 114 (E10), E10001.
Kirchoff, M.R., Grimm, R.E., 2018. Timing and distribution of single-layered ejecta craters imply sporadic preservation of tropical subsurface ice on Mars. J. Geophys. Res. Planets. 123 (1), 131–144.
Kirchoff, M.R., Grimm, R.J., Riggs, D., 2021. Preliminary examination of the spatial and temporal distribution of equatorial layered and radial ejecta craters on Mars. In: 52nd Lunar and Planetary Science Conference. The Woodlands, Texas, p. 1536.
Kneissl, T., van Gasselt, S., Neukum, G., 2011. Map-projection-independent crater size-frequency determination in GIS environments—new software tool for ArcGIS. Planet. Space Sci. 59 (11), 1243–1254.
Kress, A.M., Head, J.W., 2008. Ring-mold craters in lineated valley fill and lobate debris aprons on Mars: evidence for subsurface glacial ice. Geophys. Res. Lett. 35 (23), L23206.
Kurokawa, H., Sato, M., Ushioda, M., Matsuyama, T., Moriwaki, R., Dohm, J.M., Usui, T., 2014. Evolution of water reservoirs on Mars: constraints from hydrogen isotopes in martian meteorites. Earth Planet. Sci. Lett. 394, 179–185.
Kuzmin, R.O., Bobina, N.N., Zabalueva, E.V., Shashkina, V.P., 1988. Inhomogeneities in the upper levels of the Martian cryolithosphere. In: 19th Lunar and Planetary Science Conference. Houston, Texas, pp. 655–656.
Lagain, A., Bouley, S., Baratoux, D., Marmo, C., Costard, F., Delaa, O., Pio Rossi, A., Minin, M., Benedix, G.K., Ciocco, M., Bedos, B., Guimpier, A., Dehouck, E., Loizeau, D., Bouquety, A., Zhao, J., Vialatte, A., Cormau, M., Le Conte des Floris, E., Schmidt, F., Thollot, P., Champion, J., Martinot, M., Gargani, J., Beck, P., Boisson, J., Paulien, N., Séjourné, A., Pasquon, K., Christoff, N., Belgacem, I., Landais, F., Rousseau, B., Dupeyrat, L., Franco, M., Andrieu, F., Cecconi, B., Erard, S., Jabaud, B., Malarewicz, V., Beggiato, G., Janez, G., Elbaz, L., Ourliac, C., Catheline, M., Fries, M., Karamoko, A., Rodier, J., Sarian, R., Gillet, A., Girard, S., Pottier, M., Strauss, S., Chanon, C., Lavaud, P., Boutaric, A., Savourat, M., Garret, E., Leroy, E., Geffray, M.C., Parquet, L., Delagoutte, M.A., Gamblin, O., 2021. Mars crater database: a participative project for the classification of the morphological characteristics of large Martian craters. In: Reimold, W.U., Koeberl, C. (Eds.), Large Meteorite Impacts and Planetary Evolution VI. Geological Society of America, pp. 629–644.
Lammer, H., Kolb, C., Penz, T., Amerstorfer, U.V., Biernat, H.K., Bodiselitsch, B., 2003. Estimation of the past and present Martian water-ice reservoirs by isotopic constraints on exchange between the atmosphere and the surface. Int. J. Astrobiol. 2 (3), 195–202.
Lange, L., Forget, F., Vincendon, M., Spiga, A., Vos, E., Aharonson, O., Millour, E., Bierjon, A., Vandemeulebrouck, R., 2023. A reappraisal of subtropical subsurface water ice stability on Mars. Geophys. Res. Lett. 50 (21), e2023GL105177.
Laskar, J., Correia, A.C.M., Gastineau, M., Joutel, F., Levrard, B., Robutel, P., 2004. Long term evolution and chaotic diffusion of the insolation quantities of Mars. Icarus 170 (2), 343–364.
Lauro, S.E., Pettinelli, E., Caprarelli, G., Guallini, L., Rossi, A.P., Mattei, E., Cosciotti, B., Cicchetti, A., Soldovieri, F., Cartacci, M., Di Paolo, F., Noschese, R., Orosei, R., 2021. Multiple subglacial water bodies below the south pole of Mars unveiled by new MARSIS data. Nat. Astron. 5 (1), 63–70.
Li, C., Zheng, Y., Wang, X., Zhang, J., Wang, Y., Chen, L., Zhang, L., Zhao, P., Liu, Y., Lv, W., Liu, Y., Zhao, X., Hao, J., Sun, W., Liu, X., Jia, B., Li, J., Lan, H., Fa, W., Pan, Y., Wu, F., 2022. Layered subsurface in Utopia Basin of Mars revealed by Zhurong rover radar. Nature 610, 308–312.
Lunine, J.I., Chambers, J., Morbidelli, A., Leshin, L.A., 2003. The origin of water on Mars. Icarus 165 (1), 1–8.
Malakhov, A.V., Mitrofanov, I.G., Golovin, D.V., Litvak, M.L., Sanin, A.B., Djachkova, M. V., Lukyanov, N.V., 2022. High resolution map of water in the Martian regolith observed by FREND neutron telescope onboard ExoMars TGO. J. Geophys. Res. Planets. 127 (5), e2022JE007258.
Malin, M.C., Edgett, K.S., 1999. Oceans or seas in the Martian northern lowlands: high resolution imaging tests of proposed coastlines. Geophys. Res. Lett. 26 (19), 3049–3052.
Mellon, M.T., Jakosky, B.M., 1993. Geographic variations in the thermal and diffusive stability of ground ice on Mars. J. Geophys. Res. Planets. 98 (E2), 3345–3364.
Mellon, M.T., Sizemore, H.G., 2022. The history of ground ice at Jezero crater Mars and other past, present, and future landing sites. Icarus 371, 114667.
Melosh, H.J., 1989. Impact Cratering: A Geologic Process. Oxford University Press, New York.
Meresse, S., Costard, F., Mangold, N., Masson, P., Neukum, G., 2008. Formation and evolution of the chaotic terrains by subsidence and magmatism: Hydraotes Chaos, Mars. Icarus 194 (2), 487–500.
Mitrofanov, I., Anfimov, D., Kozyrev, A., Litvak, M., Sanin, A., Tret'yakov, V., Krylov, A., Shvetsov, V., Boynton, W.v., Shinohara, C., 2002. Maps of subsurface hydrogen from the high energy neutron detector, Mars Odyssey. Science 297 (5578), 78–81.
Mitrofanov, I., Malakhov, A., Djachkova, M., Golovin, D., Litvak, M., Mokrousov, M., Sanin, A., Svedhem, H., Zelenyi, L., 2022. The evidence for unusually high hydrogen abundances in the central part of Valles Marineris on Mars. Icarus 374, 114805.
Morgan, G.A., Putzig, N.E., Perry, M.R., Bramson, A.M., Petersen, E.I., Bain, Z.M., Mastrogiuseppe, M., Baker, D.M.H., Smith, I.B., Hoover, R.H., Sizemore, H.G., Campbell, B.A., 2019. The Mars Subsurface Water Ice Mapping (SWIM) project. In: 50th Lunar and Planetary Science Conference. The Woodlands, Texas, p. 2918.

Morgan, G.A., Putzig, N.E., Perry, M.R., Sizemore, H.G., Bramson, A.M., Petersen, E.I., Bain, Z.M., Baker, D.M.H., Mastrogiuseppe, M., Hoover, R.H., Smith, I.B., Pathare, A., Dundas, C.M., Campbell, B.A., 2021. Availability of subsurface water-ice resources in the northern mid-latitudes of Mars. Nat. Astron. 5 (3), 230–236.
Mouginis-Mark, P., 1979. Martian fluidized crater morphology: variations with crater size, latitude, altitude, and target material. J. Geophys. Res. Solid Earth 84 (B14), 8011–8022.
Mouginot, J., Pommerol, A., Beck, P., Kofman, W., Clifford, S.M., 2012. Dielectric map of the Martian northern hemisphere and the nature of plain filling materials. Geophys. Res. Lett. 39 (2), L02202.
Mustard, J.F., 2019. Chapter 8 - sequestration of volatiles in the Martian crust through hydrated minerals: A significant planetary reservoir of water. In: Filiberto, J., Schwenzer, S.P. (Eds.), Volatiles in the Martian Crust. Elsevier, pp. 247–263.
Oehler, D.Z., Allen, C.C., 2010. Evidence for pervasive mud volcanism in Acidalia Planitia, Mars. Icarus 208 (2), 636–657.
Orosei, R., Lauro, S.E., Pettinelli, E., Cicchetti, A., Coradini, M., Cosciotti, B., Di Paolo, F., Flamini, E., Mattei, E., Pajola, M., Soldovieri, F., Cartacci, M., Cassenti, F., Frigeri, A., Giuppi, S., Martufi, R., Masdea, A., Mitri, G., Nenna, C., Noschese, R., Restano, M., Seu, R., 2018. Radar evidence of subglacial liquid water on Mars. Science 361 (6401), 490–493.
Osinski, G.R., Tornabene, L.L., Grieve, R.A.F., 2011. Impact ejecta emplacement on terrestrial planets. Earth Planet. Sci. Lett. 310 (3), 167–181.
Pathare, A.V., Feldman, W.C., Prettyman, T.H., Maurice, S., 2018. Driven by excess? Climatic implications of new global mapping of near-surface water-equivalent hydrogen on Mars. Icarus 301, 97–116.
Picardi, G., Biccari, D., Seu, R., Plaut, J., Johnson, W.T.K., Jordan, R.L., Safaeinili, A., Gurnett, D.A., Huff, R., Orosei, R., Bombaci, O., Calabrese, D., Zampolini, E., 2004. MARSIS: Mars advanced radar for subsurface and ionosphere sounding. In: Wilson, A. (Ed.), Mars Express: The Scientific Payload. ESA Publications Division, ESTEC, Noordwijk, The Netherlands.
Piqueux, S., Buz, J., Edwards, C.S., Bandfield, J.L., Kleinböhl, A., Kass, D.M., Hayne, P.O., MCS, T., Teams, T., 2019. Widespread shallow water ice on Mars at high latitudes and midlatitudes. Geophys. Res. Lett. 46 (24), 14290–14298.
Plaut, J.J., Picardi, G., Safaeinili, A., Ivanov, A.B., Milkovich, S.M., Cicchetti, A., Kofman, W., Mouginot, J., Farrell, W.M., Phillips, R.J., Clifford, S.M., Frigeri, A., Orosei, R., Federico, C., Williams, I.P., Gurnett, D.A., Nielsen, E., Hagfors, T., Heggy, E., Stofan, E.R., Plettemeier, D., Watters, T.R., Leuschen, C.J., Edenhofer, P., 2007. Subsurface radar sounding of the south polar layered deposits of Mars. Science 316 (5821), 92–95.
Putzig, N.E., Morgan, G.A., Sizemore, H.G., Hollibaugh Baker, D.M., Petersen, E.I., Pathare, A.V., Dundas, C.M., Bramson, A.M., Courville, S.W., Perry, M.R., Nerozzi, S., Bain, Z.M., Hoover, R.H., Campbell, B.A., Mastrogiuseppe, M., Mellon, M.T., Seu, R., Smith, I.B., 2023. Ice resource mapping on Mars. In: Badescu, V., Zacny, K., Bar-Cohen, Y. (Eds.), Handbook of Space Resources. Springer International Publishing, Cham, pp. 583–616.
Reiss, D., Hauber, E., Michael, G., Jaumann, R., Neukum, G., the, H.C.-I.T., 2005. Small rampart craters in an equatorial region on Mars: implications for near-surface water or ice. Geophys. Res. Lett. 32 (10), L10202.
Riu, L., Carter, J., Poulet, F., Cardesín-Moinelo, A., Martin, P., 2023. Global surficial water content stored in hydrated silicates at Mars from OMEGA/MEx. Icarus 398, 115537.
Robbins, S.J., Hynek, B.M., 2012a. A new global database of Mars impact craters $\geq$ 1 km: 1. Database creation, properties, and parameters. J. Geophys. Res. Planets. 117 (E5), E05004.
Robbins, S.J., Hynek, B.M., 2012b. A new global database of Mars impact craters $\geq$ 1 km: 2. Global crater properties and regional variations of the simple-to-complex transition diameter. J. Geophys. Res. Planets. 117 (E6), E06001.
Rummel, J.D., Beaty, D.W., Jones, M.A., Bakermans, C., Barlow, N.G., Boston, P.J., Chevrier, V.F., Clark, B.C., de Vera, J.P., Gough, R.V., Hallsworth, J.E., Head, J.W., Hipkin, V.J., Kieft, T.L., McEwen, A.S., Mellon, M.T., Mikucki, J.A., Nicholson, W.L., Omelon, C.R., Peterson, R., Roden, E.E., Sherwood Lollar, B., Tanaka, K.L., Viola, D., Wray, J.J., 2014. A new analysis of Mars "special regions": findings of the second MEPAG special regions science analysis group (SR-SAG2). Astrobiology 14 (11), 887–968.
Saberi, A.A., 2020. Evidence for an ancient sea level on Mars. Astrophys. J. Lett. 896 (2), L25.
Scheller, E.L., Ehlmann, B.L., Hu, R., Adams, D.J., Yung, Y.L., 2021. Long-term drying of Mars by sequestration of ocean-scale volumes of water in the crust. Science 372 (6537), 56–62.
Schultz, P.H., Gault, D.E., 1979. Atmospheric effects on Martian ejecta emplacement. J. Geophys. Res. Solid Earth 84 (B13), 7669–7687.
Schwenzer, S.P., Kring, D.A., 2009. Impact-generated hydrothermal systems capable of forming phyllosilicates on Noachian Mars. Geology 37 (12), 1091–1094.
Senft, L.E., Stewart, S.T., 2008. Impact crater formation in icy layered terrains on Mars. Meteorit. Planet. Sci. 43 (12), 1993–2013.
Seu, R., Phillips, R.J., Biccari, D., Orosei, R., Masdea, A., Picardi, G., Safaeinili, A., Campbell, B.A., Plaut, J.J., Marinangeli, L., Smrekar, S.E., Nunes, D.C., 2007. SHARAD sounding radar on the Mars reconnaissance orbiter. J. Geophys. Res. Planets. 112 (E5), E05S05.
Skinner, J.A., Mazzini, A., 2009. Martian mud volcanism: terrestrial analogs and implications for formational scenarios. Mar. Pet. Geol. 26 (9), 1866–1878.
Smith, D.E., Zuber, M.T., Frey, H.V., Garvin, J.B., Head, J.W., Muhleman, D.O., Pettengill, G.H., Phillips, R.J., Solomon, S.C., Zwally, H.J., Banerdt, W.B., Duxbury, T.C., Golombek, M.P., Lemoine, F.G., Neumann, G.A., Rowlands, D.D., Aharonson, O., Ford, P.G., Ivanov, A.B., Johnson, C.L., McGovern, P.J., Abshire, J.B., Afzal, R.S., Sun, X., 2001. Mars orbiter laser altimeter: experiment summary after the first year of global mapping of Mars. J. Geophys. Res. Planets. 106 (E10), 23689–23722.
Smith, P.H., Tamppari, L.K., Arvidson, R.E., Bass, D., Blaney, D., Boynton, W.V., Carswell, A., Catling, D.C., Clark, B.C., Duck, T., DeJong, E., Fisher, D., Goetz, W., Gunnlaugsson, H.P., Hecht, M.H., Hipkin, V., Hoffman, J., Hviid, S.F., Keller, H.U., Kounaves, S.P., Lange, C.F., Lemmon, M.T., Madsen, M.B., Markiewicz, W.J., Marshall, J., McKay, C.P., Mellon, M.T., Ming, D.W., Morris, R.V., Pike, W.T., Renno, N., Staufer, U., Stoker, C., Taylor, P., Whiteway, J.A., Zent, A.P., 2009. H_2O at the phoenix landing site. Science 325 (5936), 58–61.
Stone, S.W., Yelle, R.V., Benna, M., Lo, D.Y., Elrod, M.K., Mahaffy, P.R., 2020. Hydrogen escape from Mars is driven by seasonal and dust storm transport of water. Science 370 (6518), 824–831.
Stuurman, C., Osinski, G., Holt, J., Levy, J., Brothers, T., Kerrigan, M., Campbell, B., 2016. SHARAD detection and characterization of subsurface water ice deposits in Utopia Planitia, Mars. Geophys. Res. Lett. 43 (18), 9484–9491.
Sun, Z., 2022. Prospect of Mars exploration and sample return. In: Deep Space Exploration and Extraterrestrial Survival Technology Forum. Nanjing, China.
Tanaka, K.L., 1997. Sedimentary history and mass flow structures of Chryse and Acidalia Planitiae, Mars. J. Geophys. Res. Planets. 102 (E2), 4131–4149.
Tanaka, K., Robbins, S., Fortezzo, C., Skinner, J., Hare, T., 2014. The digital global geologic map of Mars: chronostratigraphic ages, topographic and crater morphologic characteristics, and updated resurfacing history. Planet. Space Sci. 95, 11–24.
Villanueva, G.L., Mumma, M.J., Novak, R.E., Käufl, H.U., Hartogh, P., Encrenaz, T., Tokunaga, A., Khayat, A., Smith, M.D., 2015. Strong water isotopic anomalies in the martian atmosphere: probing current and ancient reservoirs. Science 348 (6231), 218–221.
Viola, D., McEwen, A.S., Dundas, C.M., Byrne, S., 2015. Expanded secondary craters in the Arcadia Planitia region, Mars: evidence for tens of Myr-old shallow subsurface ice. Icarus 248, 190–204.
Watters, T.R., Campbell, B.A., Leuschen, C.J., Morgan, G.A., Cicchetti, A., Orosei, R., Plaut, J.J., 2024. Evidence of ice-rich layered deposits in the Medusae fossae formation of Mars. Geophys. Res. Lett. 51 (2), e2023GL105490.
Weiss, D.K., Head, J.W., 2013. Formation of double-layered ejecta craters on Mars: a glacial substrate model. Geophys. Res. Lett. 40 (15), 3819–3824.
Wernicke, L.J., Jakosky, B.M., 2021. Martian hydrated minerals: a significant water sink. J. Geophys. Res. Planets. 126 (3), e2019JE006351.
Wilson, J.T., Eke, V.R., Massey, R.J., Elphic, R.C., Feldman, W.C., Maurice, S., Teodoro, L.F.A., 2018. Equatorial locations of water on Mars: improved resolution maps based on Mars Odyssey Neutron Spectrometer data. Icarus 299, 148–160.
Woronow, A., 1981. Preflow stresses in Martian rampart ejecta blankets: a means of estimating the water content. Icarus 45 (2), 320–330.
Xiao, L., Huang, J., Kusky, T., Head, J.W., Zhao, J., Wang, J., Wang, L., Yu, W., Shi, Y., Wu, B., Qian, Y., Huang, Q., Xiao, X., 2023. Evidence for marine sedimentary rocks in Utopia Planitia: Zhurong rover observations. Natl. Sci. Rev. 10 (9), nwad137.
Zhu, K., Schiller, M., Pan, L., Saji, N.S., Larsen, K.K., Amsellem, E., Rundhaug, C., Sossi, P., Leya, I., Moynier, F., Bizzarro, M., 2022. Late delivery of exotic chromium to the crust of Mars by water-rich carbonaceous asteroids. Sci. Adv. 8 (46), eabp8415.